

Development of Inspection and Repair Technology for Heat Exchanger Tubes in Fast Breeder Reactors

Akihiko NISHIMURA^{*1}, Takahisa SHOBU, Kiyoshi OKA, Toshihiko YAMAGUCHI,

Yukihiro SHIMADA, Obideu MIHALACHE, Akihiro TAGAWA and Takuya YAMASHITA

^{*1} Japan Atomic Energy Agency, 8-1 Umebidai Kizugawa, Kyoto 619-0215, Japan
E-mail: nishimura.akihiko@jaea.go.jp

A prototype probe system with a hybrid optical fiber scope was designed for inspecting and repairing heat exchanger tubes in fast breeder reactors (FBRs). It comprises a laser processing head combined with an eddy current testing unit. Ultrashort laser pulse ablation is used to remove work-hardened layers. And spot laser welding is used to repair cracks. This system is both a safe and economical option for the maintenance of FBRs because it extends the lifetime of the heat exchangers.

Keywords: maintenance, heat exchanger tube, hybrid optical fiber scope, laser welding, eddy current testing, laser ablation, X-ray stress measurement

1. Introduction

At present, laser material processing is widely used to fabricate precision industrial products such as electronic devices and mechanical parts on actual industrial lines. Laser material processing can also be applied in the maintenance of large structures such as nuclear reactors and chemical factories [1]. Internal access to a blanket cooling pipe with a bend section is inevitably required in D-T burning reactors such as the International Thermonuclear Experimental Reactor (ITER). At the JAEA, an internal-access pipe welding/cutting/inspection tool for manifolds and branch pipes was developed for this purpose [2,3]. Here, the design concept of the welding/cutting/inspection processing head with a composite-type flexible optical fiber was presented for welding, cutting and close observation. This tool allowed effective inspection in observation. Then, it succeeded to cut and weld branch pipes up to 50 mm in diameter.

Laser peening has been found to be effective in maintaining nuclear reactors. The second harmonic pulses of nanosecond YAG lasers can induce compressive residual stresses at the surface layers in water. This has become an indispensable technique for better prevention of stress corrosion cracking (SCC) in reactor core shrouds and containment vessels [4]. In a more recent investigation, it was demonstrated that ultrashort laser ablation also results in good prevention of SCC in stainless steel [5]. The ablation experiments were carried out in a shield of argon gas. In this study, hardened thin layers mechanically induced by a milling machine were successfully removed by ultrashort laser ablation without thermal damage.

In order to detect SCC or any other defects on the inner surface of heat exchanger tubes, eddy current testing (ECT) probes have been developed [6]. At the JAEA, the ECT probe used to detect defects in helical heating tubes in the fast breeder reactor (FBR) "Monju" was specially designed and tested using a mock-up heat exchanger facility [7]. The

present ECT probe is limited to the detection of cracking on the helical heating tubes. After detection, the cracks in the tubes are regularly plugged. Hence, the development of inspection and repair technologies to extend the lifetime of FBR heat exchanger units is indispensable.

This report describes a new probe system with laser processing, which is able to access heat exchanger tubes for maintenance. First, ultrashort laser ablation was tested on stainless steel for residual stress measurement in order to examine its validity. Second, the original concept, combining a composite-type optical fiberscope and a laser processing head with an ECT unit, is presented. This system was designed to be inserted into FBR heat exchanger tubes for inspection and repair.

2. Laser ablation experiment

In previous work, ultrashort laser pulses were typically irradiated to ablate a 2-mm-square cubic sample surface [5]. The cubic sample was cut into two pieces to measure hardness distribution along the depth with a Vickers hardness tester. The following experiment uses a larger area of 1×10 cm, where the number of scanning cycles and the laser spot diameter were tested. The area of 1×10 cm is equal to the circumference length of the laser-welded joint sections of FBR heat exchanger tubes.

2.1 Sample preparation and laser system

The sample material was 304L austenitic stainless steel. After a steel plate had been annealed, a milling machine artificially reproduced work-hardened layers on it. Then the steel plate was cut and sliced into samples of 200×100 mm in size with a thickness of 5 mm. Laser ablation was carried out on the surface of each sample. A Ti:Sapphire Chirped Pulse Amplification laser (Thales Laser $\alpha 10$) was used. A laser pulse duration of 50 fs with pulse energy of 27 mJ was focused by a 50 mm focal length plane-concave

Report Documentation Page

Form Approved
OMB No. 0704-0188

Public reporting burden for the collection of information is estimated to average 1 hour per response, including the time for reviewing instructions, searching existing data sources, gathering and maintaining the data needed, and completing and reviewing the collection of information. Send comments regarding this burden estimate or any other aspect of this collection of information, including suggestions for reducing this burden, to Washington Headquarters Services, Directorate for Information Operations and Reports, 1215 Jefferson Davis Highway, Suite 1204, Arlington VA 22202-4302. Respondents should be aware that notwithstanding any other provision of law, no person shall be subject to a penalty for failing to comply with a collection of information if it does not display a currently valid OMB control number.

1. REPORT DATE JUN 2009		2. REPORT TYPE		3. DATES COVERED 00-00-2009 to 00-00-2009	
4. TITLE AND SUBTITLE Development of Inspection and Repair Technology for Heat Exchanger Tubes in Fast Breeder Reactors				5a. CONTRACT NUMBER	
				5b. GRANT NUMBER	
				5c. PROGRAM ELEMENT NUMBER	
6. AUTHOR(S)				5d. PROJECT NUMBER	
				5e. TASK NUMBER	
				5f. WORK UNIT NUMBER	
7. PERFORMING ORGANIZATION NAME(S) AND ADDRESS(ES) Japan Atomic Energy Agency,8-1 Umehidai Kizugawa,Kyoto 619-0215, Japan,				8. PERFORMING ORGANIZATION REPORT NUMBER	
9. SPONSORING/MONITORING AGENCY NAME(S) AND ADDRESS(ES)				10. SPONSOR/MONITOR'S ACRONYM(S)	
				11. SPONSOR/MONITOR'S REPORT NUMBER(S)	
12. DISTRIBUTION/AVAILABILITY STATEMENT Approved for public release; distribution unlimited					
13. SUPPLEMENTARY NOTES See also ADM002324. Presented at the International Congress on Laser Advanced Materials Processing (5th) (LAMP 2009) Held in Kobe, Japan on June 29-July 2, 2009. Sponsored by AFOSR/AOARD. U.S. Government or Federal Rights License.					
14. ABSTRACT					
15. SUBJECT TERMS					
16. SECURITY CLASSIFICATION OF:			17. LIMITATION OF ABSTRACT Same as Report (SAR)	18. NUMBER OF PAGES 5	19a. NAME OF RESPONSIBLE PERSON
a. REPORT unclassified	b. ABSTRACT unclassified	c. THIS PAGE unclassified			

lens on the plate in air. During laser irradiation, the sample was fixed on a holder having a 3D motion-controlled stage.

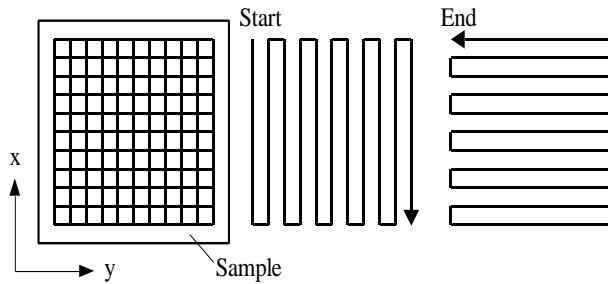


Fig. 1 Scheme of laser pulse scanning

The relation between the laser scanning directions is shown in Fig. 1. One scanning cycle means that the scanning in the x-direction begins from “start” and then the scanning in the y-direction returns to “end.” Each scan has a 1 mm shift at the return. One scanning cycle takes 131 seconds. Table 1 shows the combination of the number of scanning cycles and the spot diameter on the sample surface. Nine laser-processed samples and one reference sample without laser processing were prepared.

Table 1 Conditions for laser ablation.

		Number of scanning cycles			
		0	1	3	7
Spot diameter, mm	0.3	No. 0	No. 1	No. 2	No. 3
	0.6		No. 4	No. 5	No. 6
	0.9		No. 7	No. 8	No. 9

2.2 Microscopic observations

Figure 2 shows selected pictures of the sample surfaces, measured by an optical microscope. Machining has left its traces on the sample surface shown in Fig. 2(a). The picture area is 2×1.5 mm. The horizontally machined traces have spacings of approximately 0.6 mm. The traces were like grooves on optical gratings, which were exposed to laser irradiation.

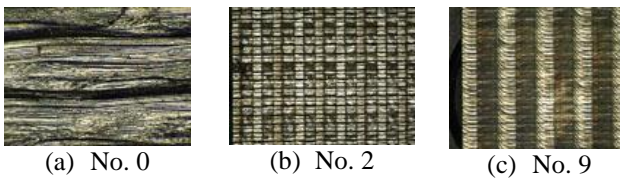


Fig. 2 Microscopic views of SUS304 sample surface

The scheme of the laser pulse scanning created a zebra pattern. Figures 2(b) and 2(c) show the sample surfaces after laser irradiation. Each one has the area of 11×7 mm. In Fig. 2(b), the number of scanning cycles is 3. The characteristic zebra pattern appears in the case of a spot diameter of 0.3 mm. This is because the periodic scanning has induced repetitive oxidization and ablation with deposition

of oxide microparticles. In Fig. 2(c), the number of scanning cycles is 7 with a spot diameter of 0.9 mm.

As the spot diameter increases, the zebra patterns become wider and more obscure. The depths of the initial traces gradually become shallower as the number of scanning cycles increases.

3. Design concept of a new probe system for FBR heat exchanger tubes

In order to apply the abovementioned laser processing for the maintenance of the heat exchanger units, it is very important to be able to access the inner walls of the heat exchanger tubes. The heat exchanger consists of an evaporator and a superheater. In the evaporator, the outer diameter of the tubes is 31.8 mm. The material used for the evaporator is steel with 2.25% chromium and a thickness of 3.8 mm. In the superheater, 3.5-mm-thick stainless steel 321 is used. The length of the evaporator is 85 m and that of the superheater is 47 m. The tube has a helical shape with a radius of 1.2–2.7 m. The minimum radius around the inlet/outlet is 0.16 m.

In the evaporator, there is both boiling water and steam in the heat exchanger tubes. The transit position from water to steam depends on the operational temperature of the liquid sodium coolant. The inner surface of the tube turns into an oxide layer of magnetite that can prevent further erosion. The steam generated in the evaporator is supplied to the superheater where it is heated under dry conditions. If even a tiny amount hot water leaks and comes into contact with liquid sodium, it could seriously damage the heat exchanger unit; this would result in immediate suspension of the power plant operation. From the perspective of risk assessment, more attention should be given to the detection of erosion symptoms in the evaporator than in the superheater.

The prototype probe system should be able to inspect the inner wall of a 1-inch-diameter tube that is covered with a magnetite layer. The prototype system was designed to use a composite-type optical fiberscope, which delivers processing laser pulses and provides images of the repaired inner wall.

3.1 Composite-type optical fiberscope

Endoscopic techniques have been widely used in minimally-invasive abdominal surgical procedures because only a few keyhole incisions are required. The use of a composite-type optical fiber reduces the risk of a surgeon perceiving a gap between the center of his view and the direction of the laser beam.

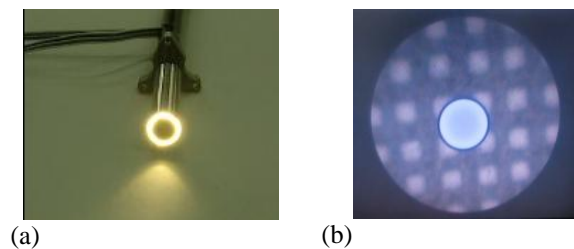


Fig. 3 Composite-type optical fiber
(a) telescope section, (b) image view of 0.15 mm mesh

Figure 3(a) shows the telescope section of a composite-type optical fiber. The telescope, which relays images from the inner surface to the edge of the optical fiber, consists of quartz lenses in a stainless steel sleeve. The fiber is made of synthetic quartz with three cylindrical structures. Each structure has its own function. A 0.2-mm-diameter center fiber delivers the processing high-energy laser beam. Image fibers, which deliver the visible image for the endoscope, surround the center fiber. The picture elements of the endoscope are laid parallel like a honeycomb and can directly send images from one end to another. There are 20,000 image fibers, so the processing images are transmitted with high clarity and resolution. Light guide fibers, which supply illumination intensity, are located on the outer side of the image fibers. The total length of the composite-type optical fiber is 10 m. Figure 3(b) shows a view of 0.15 mm mesh through the telescope.

The composite-type optical fiberscope was originally developed for inspecting and repairing the robot system for tritium breeder blankets in an ITER project. It was improved for application as a surgical device for low infestation treatment [8].

3.2 Laser processing head

The laser processing head was specifically designed to access the inner walls of heat exchanger tubes. It comprises a movable sleeve that is driven by two pulse motors. Both rotational and longitudinal motion are possible on the sleeve, which has a 45° tilted mirror at the inside end and an oval hole where a high-energy laser beam and images are transmitted. Figure 4 is a photograph of the laser processing head inserted in a 1-inch acrylic pipe. The outer diameter was designed to be less than 20 mm. The movable sleeve is supported by ball bearings in a housing, which make it possible to move the processing head 5 mm in the longitudinal direction and rotate it by $\pm 185^\circ$.



Fig. 4 Laser processing head

3.3 ECT sensor and measurement system

ECT is now widely used in many manufacturing and service environments that require inspection of thin metal for safety-related problems. In the nuclear engineering industry, ECT can be used for certain metal thickness measurements to determine the existence of cracks in metal sheets and tubing. ECT has several advantages over ultrasonic transducer testing. For example, ECT can examine large areas very quickly and it does not require coupling liquids between the sensor and the specimens. Since hundreds of heat exchanger tubes in the heat exchanger units of nuclear power plants require inspection, it is very important to reduce the time of each examination.



Fig. 5 ECT sensor units

Figure 5 is a photograph of the ECT sensor units. To increase the resolution and penetration of this ECT probe system, both a center coil and a pair of induction coils were prepared. The multiple detection coils were placed close to the inner wall of the center unit. Here, 20 detection coils were molded in a plastic hollow mount. One channel consists of a pair of coils so that 10 channels can be applied. When a crack in the inner wall disturbs the eddy current circulation, the magnetic coupling with the detection coils is changed and a defect signal can be read by coil impedance variation. The detection signals are amplified by lock-in amplifiers and are transferred to analog/digital (A/D) converters. In addition, a pair of induction coils induces an intense eddy current with low frequency. The use of the center coil and induction coils is called “remote field,” and is provided for detecting cracks in the outer side of the heat exchanger tubes.

3.4 Coupling device

The function of the coupling device is to axially combine the processing laser beam and the images of the inner tube walls. Figure 6 shows the inside view of the coupling device housing. A laser beam supplied with a QBH connector goes into a laser beam collimator. The collimator was specifically designed for the NA value of the laser beam. A dielectric coating mirror at a 45° angle reflects the 1.07- μm collimated laser beam to a focusing lens. At the end of the composite-type optical fiber, the collimated laser beam is focused on its center core fiber at a 0.2-mm diameter. Visible light coming from the composite-type optical fiber faces in the opposite direction and goes through the dielectric coating mirror to a charge-coupled device (CCD) camera. Reflection loss on the optical components in the coupling device was designed to be less than 10%. Temperature rise is monitored by thermocouples. The housing of the coupling device is sealed and the micro particle density is monitored.

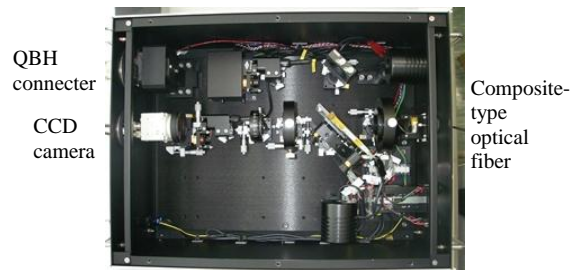


Fig. 6 Inside view of the coupling device housing

4. Results and discussion

4.1 Laser ablation and peening

A milled surface has a hardened thin layer with residual tensile stress, which is sensitive to SCC susceptibility. Ultrashort laser ablation is useful to remove the hardened thin

layer [4] and can be applied for mitigation against SCC. However, improvement of internal residual stress has not yet been clarified. In the present study, stress measurements were performed on the laser ablation samples. The synchrotron radiation X-ray in BL22XU at SPring-8 was applied [9]. The energy of the X-ray was 66.84 keV, which is capable of detecting internal residual stress distribution. The stress distribution from the surface to the depth of 0.15 mm was observed using a strain scanning method with a Ge (111) analyzer [10].

Figure 7 shows that the surface to the depth of 0.05 mm has high tensile residual stress. The improvement for residual stress is not significantly effective, as shown in the plots of No. 2 and No. 5. However, the improvement for residual stress becomes effective in the plots of No. 8 and No. 9. For No. 2 and No. 5, the laser spot diameter is equal to or less than the trace spacing of 0.6 mm or the scanning shift of 1 mm. The residual stress distribution was improved at the laser spot diameter of 0.9 mm at No. 8. Further improvement was achieved as the number of scanning cycles reached 7 at No. 9. It shows the compressive residual stress condition at the depth of approximately 0.05–0.07 mm. Most of the hardened layers were ablated by ultrashort laser irradiation. During free expansion, the solid density plasma compressed the target on the order of tens of GPa. High pressure with ultrashort time duration enables the generation of intense shockwaves and freezes the iron phase in the nonequilibrium state [11]. Here, the residual compressed stress is also apparent evidence of high pressure. For laser peening in industrial applications, frequency doubling Q-switched YAG laser pulses in water have been commonly used. The ultrashort laser ablation has similar effects even in dry condition.

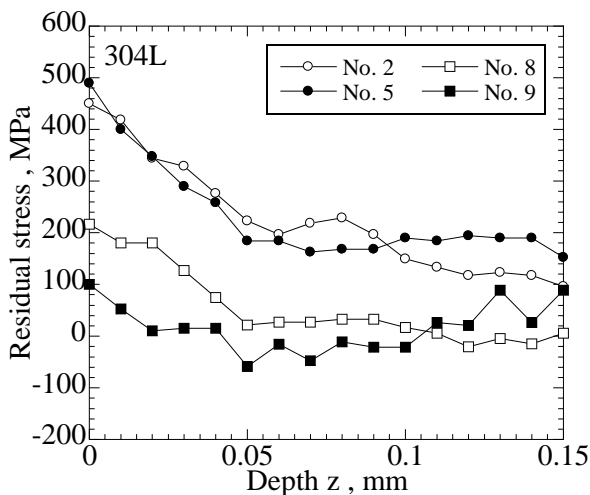


Fig. 7 Distribution of residual stress

4.2 Crack detection

The ECT method was improved to survey the heat exchanger units of FBR “Monju” which has three independent cooling loops within the heat exchanger units. At the present time, there are no defects or cracks on the heat exchanger tubes of any of the loops. Careful inspection will continue into the future. The following paragraph refers to ECT performance using an artificial crack.

Figure 8 is a demonstration of a detection result by the ECT sensor unit. The artificial crack was 0.5 mm wide with a 10% tube thickness, fabricated by electrical discharge machining. ECT signals from a 10-channel A/D convertor created an original waveform. Noise filters were applied to the original signal. A low pass filter reduced spiky noise and a band cut filter suppressed the periodic pattern in space. A band cut filter successfully extracted the artificial crack, as indicated by the red color in Fig. 8(a). The periodic pattern, the yellow colour, was suppressed, which was supposed to indicate the initial deformation on the heat exchanger tube. Generally speaking, the hot rolling process sometimes causes slight deformation. The software also has a function to indicate stereoscopic effect, which is shown in Fig. 8(b).

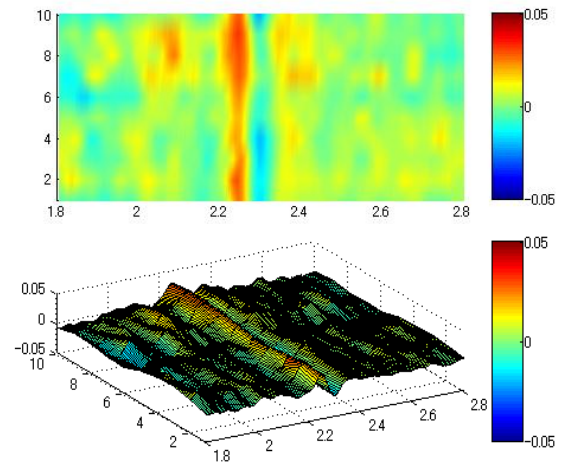


Fig. 8 ECT detection for a crack on a 1 inch diameter tube
(a) noise filtered signal, (b) stereoscopic view

4.3 Heat source for welding

High-energy electron beams have been used for melting, welding, and vaporization in nuclear energy research. For example, in Atomic Vapor Laser Isotope Separation, a high-energy electron beam successfully evaporated uranium or gadolinium metal, which had been charged in a water-cooled crucible [12]. In nuclear fusion research, plasma disruption on a divertor of JT-60 was also demonstrated by electron beam heating [13]. On the other hand, several type lasers have been used for laser welding. Recently, compact fiber lasers have been available for various material welding. They can produce high-focused intensity with a good beam profile on targets in air close to electron beam heating, which will expand the application of the laser welding [14]. In the present research, a rare earth element doped fiber laser was chosen for the new probe system. In-process monitoring and adaptive control in continuous wave laser welding was studied by a fiber laser [15]. A 100 W fiber laser carried out micro bead-on-plate welding on 0.1 mm thick stainless steel sheets on an aluminum heat sink. The bead width was 320 μm on the average 10 mm/sec welding speed. It seems that this micro welding scale is similar to that by the probe system.

Figure 9 shows a laser welding demonstration by a high power fiber laser. An ytterbium fiber laser and the composite-type optical fiberscope were connected in the

coupling device. The laser output was increased to 1 kW. The target was a STBA24 tube containing 2.25% Cr. The working distance from the fiberscope to the target was 19 mm. A shielding glass plate was set to protect the fiberscope lens. An input power of 300 W with 1 second irradiation had sufficient heat-load for spot welding. The target surface had a shallow dimple of 0.52 mm in diameter and a surrounding molten zone with a diameter of 0.87 mm. Oxide particles were deposited up to a diameter of 1.5 mm. As the input power was increased over 400 W, surface evaporation and fume generation at the molten pool became strong. Contamination on the shielding glass plate prevented a laser power of over 400 W from reaching the target surface. Therefore, it is determined that a high brilliant fiber laser of 300 W is satisfactory for spot laser welding.



Fig. 9 Molten pool on a heat exchanger tube

Some of Japan's oldest nuclear power plants are now entering their 30th year. To extend their designed lifespan up to 60 years, in-situ flaw sizing and repairs are needed [16]. The probe system for a FBR heat exchanger here presented could be useful for anti-aging mitigation on presently-operating nuclear generation plants.

5. Conclusion

A new probe system was proposed to maintain FBR heat exchanger tubes. Ultrashort pulse laser ablation was applied to the shroud material. Work-hardened layers of 1 × 10 cm SUS304 were successfully removed with reduction of tensile residual stress. A composite-type optical fiberscope was used as the backbone of the newly proposed probe system. ECT units, a laser processing head, and a coupling device were combined in the system. ECT clarified the size of the cracks for repair. A laser welding demonstration decided the output power of the fiber laser. This system will be tested at the mockup facility for heat exchanger units. This new probe system will demonstrate laser peening for the laser-welded sections of heat exchanger tubes.

Acknowledgments

The authors wish to thank Mr. Tomohiro Akatsu and Mr. Takeshi Seki for their technical assistance. The authors also wish to thank Dr. Takashi Tsukada for his valuable discussion about SCC in the boiling water reactor. And Dr. Toyoaki Kimura, Dr. Atsushi Yokoyama and Dr. Shunichi

Kawanishi kindly gave the authors their continuous support in promoting this project.

The present study includes the results of "Development of maintenance technologies with a new probe system for FBR heat exchanger tubes" entrusted to the Japan Atomic Energy Agency by the Ministry of Education, Culture, Sports, Science and Technology of Japan (MEXT).

References

- [1] M. Kutsuna, et al., "Special Issue on Recent Advanced Laser Processing Applied to Actual Industrial Lines," *The Review of Laser Engineering*, 33, (2003). (in Japanese)
- [2] K. Oka, A. Itou, Y. Takiguchi, A. Itou, *Journal of Robotics and Mechatronics*, 10, (1998), 104. (Journals)
- [3] K. Oka, E. Tada, S. Kimura, T. Ogawa and N. Sasaki, *SPIE-Proceedings*, 3888, (1999) 702. (Conference Proceedings)
- [4] Y. Sano, et al., *Proc. 8th Int. Conf. on Nuclear Engineering (ICONE-8)*, Baltimore, (2000) Paper No. 8441. (Conference Proceedings)
- [5] A. Nishimura, E. Minehara, T. Tsukada, M. Kikuchi and J. Nakano, *SPIE-Proceedings*, 5562, (2004) 673. (Conference Proceedings)
- [6] "Nondestructive Testing Handbook, Second edition Volume 4, Electromagnetic Testing" ed. by R. C. McMaster (Publisher, American Society for Nondestructive Testing) p.26. (Books)
- [7] T. Inoue, A. Sueoka, Y. Nakano, H. Kanemoto, Y. Imai and T. Yamaguchi, *Nuclear Engineering and Design*, 237, (2007) 858. (Journals)
- [8] K. Oka, *Energy Review*, 7, (2007) 7.
- [9] T. Shobu, K. Tozawa, H. Shiwaku, H. Konishi, T. Inami, T. Harami and J. Mizuki, *AIP Conference Proc.* 879 (2007), pp. 902-906. (Conference Proceedings)
- [10] T. Shobu, J. Mizuki, K. Suzuki, Y. Akiniwa and K. Tanaka, *JSME International Journal, Series A*, Vol. 49, No. 3 (2006), pp.376-381. (Journals)
- [11] T. Sano, H. Mori, E. Ohnuma and I. Miyamoto, *Appl. Phys. Lett.* 83 (2003) 3498. (Journals)
- [12] A. Nishimura, H. Ohba, K. Ogura and T. Shibata, *Opt. Commun.*, 110, (1994), 561. (Journals)
- [13] K. Nakamura, et al., *J. Nucl. Mat.*, 258, (1998) 823. 8th International conference on fusion reactor materials. (Conference Proceedings)
- [14] S. Katayama, *Journal of Japan Laser Processing Society*, 15-1, (2008), 35. (Journals)
- [15] Y. Kawahito and S. Katayama: *Proc. 69th Laser Materials Processing Conferences*, Tokyo, (2007) p.49. (Conference Proceedings)
- [16] Y. Yamashita, *J. Nucl. Sci. Tech.*, 38, (2001), 887. (Journals)